0013-7227/08/$15.00/0
Printed in U.S.A.

Endocrinology 149(10):5136–5145

doi: 10.1210/en.2008-0161

Inhibition of Cholesterol Biosynthesis Impairs Insulin Secretion and Voltage-Gated Calcium Channel Function in Pancreatic β-Cells

Fuzhen Xia, Li Xie, Anton Mihic, Xiaodong Gao, Yi Chen, Herbert Y. Gaisano, and Robert G. Tsushima

Departments of Medicine and Physiology, University of Toronto, Toronto, Ontario, Canada M5S 1A8

Insulin secretion from pancreatic β-cells is mediated by the opening of voltage-gated Ca^{2+} channels (Ca_V) and exocytosis of insulin dense core vesicles facilitated by the secretory soluble *N*-ethylmaleimide-sensitive factor attachment protein receptor protein machinery. We previously observed that β-cell exocytosis is sensitive to the acute removal of membrane cholesterol. However, less is known about the chronic changes in endogenous cholesterol and its biosynthesis in regulating β-cell stimulus-secretion coupling. We examined the effects of inhibiting endogenous β-cell cholesterol biosynthesis by using the squalene epoxidase inhibitor, NB598. The expression of squalene epoxidase in primary and clonal β-cells was confirmed by RT-PCR. Cholesterol reduction of 36–52% was observed in MIN6 cells, mouse and human pancreatic islets after a 48-h incubation with 10 μM NB598. A similar reduction in cholesterol was observed in the subcellular compartments of MIN6 cells. We found NB598 significantly inhibited both basal and glucose-stimulated insulin secretion from mouse pancreatic islets. Ca_V channels were markedly inhibited by NB598. Rapid photolytic release of intracellular caged Ca^{2+} and simultaneous measurements of the changes in membrane capacitance revealed that NB598 also inhibited exocytosis independently from Ca_V channels. These effects were reversed by cholesterol repletion. Our results indicate that endogenous cholesterol in pancreatic β-cells plays a critical role in regulating insulin secretion. Moreover, chronic inhibition of cholesterol biosynthesis regulates the functional activity of Ca_V channels and insulin secretory granule mobilization and membrane fusion. Dysregulation of cellular cholesterol may cause impairment of β-cell function, a possible pathogenesis leading to the development of type 2 diabetes. (*Endocrinology* 149: 5136–5145, 2008)

PANCREATIC β-CELLS secrete insulin in response to elevated glucose to maintain blood glucose homeostasis. Defects in β-cell insulin secretion lead to hyperglycemia and development of type 2 diabetes. The distal events underling stimulus-secretion coupling of insulin secretion have been well documented and are characterized by two major events (1). The first involves changes in electrical activity of β-cell ion channels, and the second, the function of secretory machinery regulated by the soluble *N*-ethylmaleimide-sensitive factor attachment protein receptor (SNARE) proteins.

Uptake of glucose by β-cells enhances mitochondrial oxidation and ATP production. The elevation of ATP to ADP ratio closes ATP-sensitive K^+ (K_{ATP}) channels, leading to membrane depolarization, the opening of voltage-gated Ca^{2+} (Ca_V) channels, and fusion of insulin-containing secretory granules with the plasma membrane. Voltage-gated K^+ (K_V) channels play an important role in repolarizing the membrane potential to suppress the entire process of glucose-stimulated insulin secretion (2). In this sequential glucose-stimulated insulin secretion, influx of Ca^{2+} through Ca_V channels and subsequent increase in intracellular Ca^{2+} concentration ($[Ca^{2+}]_i$) causes interaction of SNARE proteins to initiate exocytosis (3–5).

SNARE proteins play an essential role in the fusion of insulin granules with plasma membranes. vesicle-associated membrane protein (VAMP)-2 is a SNARE protein located on donor vesicles, whereas syntaxin 1A and synaptosomal-associated protein of 25 kDa (SNAP-25) are SNARE proteins located on target plasma membranes (t-SNARE). Based on the current view, SNARE proteins facilitate exocytosis by binding SNARE protein located on donor vesicles to their cognate t-SNARE proteins, giving rise to a tight complex that fuses secretory granules to plasma membranes (6, 7). SNARE protein conformational changes are believed to provide energy for membrane fusion. It is well established that glucose-stimulated insulin secretion is characterized by a biphasic pattern consisting of a transient first phase followed by a sustained second phase secretion (8). This is reflected by the sequential release of distinct pools of insulin granules; a limited readily releasable pool and a larger reserve pool, respectively (9, 10). Granules from the readily releasable pool can undergo exocytosis right after stimulation, whereas granules from the reserve pool undergo mobilization and/or priming to gain release competence, and both involve the formation of SNARE complexes (11, 12). Type 2 diabetes from human (13) and animal models (Zucker fa/fa and Goto-Kakizaki rats) (14, 15) manifest a reduced expression of

First Published Online July 3, 2008

Abbreviations: $[Ca^{2+}]_i$, Intracellular Ca^{2+} concentration; Ca_V, voltage-gated Ca^{2+} channel; Cm, membrane capacitance; ER, endoplasmic reticulum; FBS, fetal bovine serum; GFP, green fluorescence protein; K_{ATP}, ATP-sensitive K^+; KRB, Krebs-Ringer bicarbonate; K_V, voltage-gated K^+; MBS, MES-buffered saline; MβCD, methyl-β-cyclodextrin; MES, 2-(*N*-morpholine) ethane sulfonic acid; MIP, mouse insulin promoter; PM, plasma membrane; R, ratio; SG, secretory granule; SNAP-25, synaptosomal-associated protein of 25 kDa; SNARE, soluble *N*-ethylmaleimide-sensitive factor attachment protein receptor; t-SNARE, SNARE proteins located on target PMs; VAMP, vesicle-associated membrane protein.

***Endocrinology* is published monthly by The Endocrine Society (http://www.endo-society.org), the foremost professional society serving the endocrine community.**

SNARE proteins, which is partially accountable for the reduction of first-phase insulin secretion (16).

Constituting about 20% of the total membrane lipid, cholesterol is involved in several subcellular functions, such as influencing the thickness and fluidity of membranes and insulating membranes (17, 18). Cholesterol is tightly packed with sphingolipids to form specific microdomains termed membrane rafts (19, 20). Numerous membrane proteins are found to be associated with membrane rafts, in which the normal function of targeted proteins is regulated. Caveolins are constituent proteins of membrane rafts (21). We have demonstrated that ion channels ($Ca_V1.2$, $K_V2.1$) and SNARE proteins (syntaxin 1A, SNAP-25, and VAMP-2) are targeted to these cholesterol-rich membrane raft microdomains in pancreatic β- and α-cells (22, 23).

Our observations demonstrated that acute depletion of membrane cholesterol with methyl-β-cyclodextrin (MβCD) implicated the association of ion channels and SNARE proteins with membrane rafts in β- and α-cells, which plays an important role in regulating insulin and glucagon secretion. However, less is known about the effects of chronic cholesterol depletion on β-cell function. Squalene epoxidase (a flavoprotein monooxidase located on the endoplasmic reticulum) is the second enzyme in the committed cholesterol biosynthesis pathway (24). Here we demonstrate that the squalene epoxidase inhibitor, NB598, significantly inhibits endogenous cholesterol biosynthesis, resulting in impaired β-cell insulin secretion. Furthermore, we demonstrate that the mediators of this effect involve the inhibition of Ca_V channels and the impairment of the exocytotic machinery.

Materials and Methods

Cell culture

Mouse MIN6 cells (kindly provided by S. Seino, Chiba University, Chiba, Japan) were grown in monolayer and maintained in DMEM (Sigma, Oakville, Ontario, Canada) containing 25 mM glucose and supplemented with 10% fetal bovine serum, 100 U/ml penicillin, 100 μg/ml streptomycin, 2 mM [scap]l[r]-glutamine, and 0.05 mM 2-mercaptoethanol at 37 C in a humidified atmosphere (5% CO_2). Cells were passaged every 4–5 d at 80% confluence.

Pancreatic islet isolation and dispersion

Mouse pancreatic islets from mouse insulin promoter (MIP)-green fluorescence protein (GFP)-transgenic mice (kindly provided by Dr. M. Hara, University of Chicago, Chicago, IL) were isolated by collagenase digestion as described previously (22). Human islets were isolated (25) and kindly supplied by Dr. Jonathan Lakey (JDRF Human Islet Distribution Program, University of Alberta, Canada). Upon arrival, islets were immediately hand picked. For electrophysiological studies, islets were dispersed into single cells with 0.25% trypsin in Ca^{2+}- and Mg^{2+}-free Hanks' balanced salt solution (Invitrogen, Burlington, Ontario, Canada), placed onto coverslips, and cultured overnight before commencement of patch clamp experiments. Both intact islets and dispersed islet cells were cultured in RPMI 1640 (Sigma) media containing 11 mM glucose supplemented with 10% fetal bovine serum (FBS), 0.25% HEPES, 100 U/ml penicillin, and 100 μg/ml streptomycin. The cultured islet cells were used within 3 d. Mice were maintained in the pathogen-free animal facility at the University of Toronto, and all experiments were approved by the University of Toronto Animal Care Committee and conducted in accord with accepted standards of humane animal care.

RNA preparation and RT-PCR

Total RNA was isolated from cultured INS-1 and MIN6 cells and the pancreatic islets from rat, mouse, and human using Tri Reagent (Sigma) following the manufacturer's protocol. Subsequent deoxyribonuclease I (Ambion, Austin, TX) treatment was performed to remove any residual DNA contamination. One microgram of isolated RNA was reverse transcribed using Omniscript RT kit (QIAGEN, Mississauga, Ontario, Canada) according to the manufacturer's instructions. PCR was performed using Hot Start Taq DNA polymerase (Fermentas, Burlington, Ontario, Canada) with the primer pair targeting the squalene epoxidase gene (forward: 5′-AGCTATGGCAGAGCCCAAT-3′; reverse: 5′-TGGTAGATGAGAACTGGACT-3′). PCR protocol used was as follows: heat activation of polymerase at 94 C for 5 min, followed by 35 cycles of 94 C for 30 sec, 53 C for 30 sec, and 72 C for 60 sec. The amplified DNA from squalene epoxidase mRNA transcripts was visualized as a 280 bp band in a 2% agarose gel.

Subcellular fractionation of plasma membranes, endoplasmic reticulum, and insulin secretory granules

MIN6 cells (4×10^8) were cultured for 48 h at 37 C in the culture medium supplemented with 10% delipidated FBS (Cocalico Biological Inc., Reamstown, PA), in the absence or presence of 10 μM NB598. The cells were harvested and homogenized in fractionation buffers: 50 mM 2-(*N*-morpholino) ethane sulfonic acid (MES), 250 mM sucrose (pH 7.2) for plasma membrane (PM) and endoplasmic reticulum (ER); 10 mM 3[*N*-morholino]propanesulfonic acid-Tris, 270 mM sucrose (pH 6.8) for insulin secretory granules (SG). Fractionations for PM and ER were performed by sucrose density gradient ultracentrifugation established by Ramanadham *et al.* (26). Insulin secretory granules were fractionated with Histodenz (Sigma) gradient ultracentrifugation followed by Percoll (GE Healthcare, Baie d'Urfe, Quebec, Canada) purification, as established by Brunner *et al.* (27). The isolated subcellular fractions were stored at −20 C for protein concentration determination and cholesterol extraction.

Cholesterol content assay

MIN6 cells (5×10^5) or 20 pancreatic islets from mouse or human were cultured for 48 h at 37 C in the relative culture media supplemented with 10% delipidated FBS, in the absence or presence of 10 μM cholesterol biosynthesis inhibitor NB598 (Sigma). Cells and islets were collected and washed with PBS. Cholesterol was extracted by adding 50 μl of 2:1 chloroform-methanol mixture, followed by 100 μl of PBS. To extract cholesterol from subcellular fractions, 50 μl of 2:1 chloroform-methanol mixture was added to different compartments. The top water phase was removed after centrifugation for 3 min at 10,000 rpm. Cholesterol sample was dried and dissolved in 10–40 μl of immunoprecipitation buffer containing (in millimoles) 150 NaCl, 20 Tris-HCl, 5 $MgSO_4$, 1 EDTA, 1 EGTA, and 1% Triton X-100. Cholesterol content was measured using a fluorescence assay kit (Cayman Chemical Co., Ann Arbor, MI), following the manufacturer's instructions.

Insulin secretion assay

Krebs-Ringer bicarbonate (KRB) buffer containing (in millimoles) 129 NaCl, 5 $NaHCO_3$, 4.8 KCl, 1.2 KH_2PO_4, 2.5 $CaCl_2$, 2.4 $MgSO_4$, 10 HEPES, and 0.1% BSA was used for insulin secretion assay for mouse pancreatic islets. The isolated islets were cultured for 48 h at 37 C in the islet culture medium supplemented with 10% delipidated FBS, in the absence or presence of different doses of NB598. Three hours before the secretion assay, glucose concentration in the culture medium was changed to 2.8 mM to recover the islets to a basal condition. Twenty islets were washed once with KRB and preincubated for 30 min in 1 ml KRB supplemented with 1 mM glucose. The islets were then incubated for 1 h with 1 ml of fresh KRB supplemented with 1 mM glucose, and the supernatants were collected for the assay of basal insulin secretion. One milliliter KRB supplemented with 16.7 mM glucose was changed to incubate the islets for 1 h at 37 C and the supernatants collected for the assay of glucose-stimulated insulin secretion. The islets were washed with ice-cold PBS and lysed with 1 ml of 75% ethanol/0.03 N HCl, and the tissue lysates were kept for the determination of total insulin concentration. All samples were kept at −20 C until assayed for insulin using a RIA kit (Millipore Corp., St. Charles, MO) and values for released insulin in the supernatants were normalized to total islet insulin.

Electron microscopy

Isolated islets from MIP-GFP mice were cultured for 48 h at 37 C in islet culture medium supplemented with 10% delipidated FBS, in the absence or presence of 10 μM NB598. They were then fixed with a Karnovsky style fixative [4% paraformaldehyde + 2.5% glutaraldehyde in a 0.1 M cacodylate buffer with 5 mM $CaCl_2$ (pH 6.8)] for 1 h, postfixed with 1% osmium tetroxide for 30 min, and treated with 2.5% uranyl acetate for 30 min. The islets were then dehydrated using a graded series of ethanol and infiltrated with epoxy 812 resin in polyethylene capsules. A complete polymerization of the epoxy resin occurs for 48 h at 60 C. The solid epoxy resin blocks containing the islet samples were sectioned on a Reichert Ultracut E microtome to 70–90 nm thickness and collected on 200 mesh copper grids. The sections were counterstained for 15–20 min using saturated uranyl acetate, followed by Reynold's lead citrate and then examined and photographed in a Hitachi H7000 transmission electron microscope (Hitachi Limited, Tokyo, Japan) at an accelerating voltage of 75 kV.

Electrophysiology

The dispersed islet cells were cultured for 48 h at 37 C in islet culture medium supplemented with 10% delipidated FBS, in the absence or presence of different doses of NB598. Pancreatic β-cells can be easily recognized as being green due to the expression of GFP in MIP-GFP mice, which we have been characterized as possessing normal physiological function (28). Single β-cells were voltage clamped in the whole-cell configuration to measure Ca_V, K_V, and K_{ATP} currents as previously described (22, 23).

Photolysis of caged Ca^{2+} and cell capacitance measurement

Patch electrodes were pulled from 1.5-mm thin-walled borosilicate glass, coated close to the tip with orthodontic wax (Butler; Guelph, Ontario, Canada), and polished to a tip resistance of 2–4 MΩ when filled with intracellular solution. Standard bath solution for the experiments contained (in millimoles) 138 NaCl, 5.6 KCl, 1.2 $MgCl_2$, 2.6 $CaCl_2$, 5 D-glucose, and 5 HEPES (pH 7.4, adjusted with NaOH). Intracellular solution for flash experiments contained (in millimoles) 112 Cs-glutamate, 5 o-nitrophenyl EGTA (NP-EGTA), 3.7 $CaCl_2$, 2 Mg-ATP, 0.3 Na_2-GTP, and 0.2 fura-6 F (pH 7.2, adjusted with CsOH). NP-EGTA and fura-6 F were purchased from Molecular Probes (Invitrogen, Burlington, Ontario, Canada). Cell capacitance (Cm) was measured using an EPC-10 patch-clamp amplifier (HEKA, Lambrecht, Germany) controlled by the lock-in module of PULSE software. The capacitance traces were imported to IGOR Pro software (WaveMetrics, Lake Oswego, OR) for analysis. Flashes of UV light and fluorescence-excitation light were generated as described previously (29). In the flash experiments, exocytosis was elicited by photorelease of caged Ca^{2+} preloaded into the cell via the patch pipette. $[Ca^{2+}]_i$ was measured with the Ca^{2+} indicator dyes fura-6 F. $[Ca^{2+}]_i$ was determined from the ratio (R) of the fluorescence signals excited at the two wavelengths (340/380nm), following the equation (30): $[Ca^{2+}]_I = K_{eff} \times (R - R_{min})/(R_{max} - R)$, where K_{eff}, R_{min}, and R_{max} are constants obtained from intracellular calibration as previously described (29).

Membrane raft isolation

MIN6 cells were cultured for 48 h at 37 C in the culture medium supplemented with 10% delipidated FBS, in the absence or presence of 10 μM NB598. The cells were then harvested and lysed by sonication with cold 1% Triton X-100 in MES-buffered saline [MBS; 25 mM MES, 150 mM NaCl (pH 6.5), supplemented with protease inhibitors]. Lysed cells were centrifuged at 2000 rpm for 15 min at 4 C. The supernatant was diluted with equal volume of an 80% sucrose solution in MBS (with 1% Triton X-100) and placed into the bottom of an ultracentrifuge tube. A 30% and 5% sucrose in MBS were loaded on top of the sample, which was centrifuged at 49,000 rpm in a MLS-50 rotor (Beckman, Fullerton, CA) for 22 h at 4 C. Ten gradient fractions (480 μl each) were collected from the top, and 20–30 μl of each fraction were loaded onto an SDS-PAGE gel for Western blot analysis.

Immunoblotting

Western blot was performed to detect the changes of protein expression and membrane raft association of ion channels and SNARE proteins. MIN6 cell lysate or the fractions from sucrose gradient ultracentrifugation were subjected to SDS-PAGE and transferred to polyvinylidene difluoride-plus membranes (Fisher Scientific Ltd., Nepean, Ontario, Canada). Membranes were probed with the indicated primary antibodies; anti-$Ca_V1.2$ and $K_V2.1$ (Alomone Laboratories, Jerusalem, Israel), antisyntaxin 1A and SNAP-25 (Sigma), and anti-VAMP-2 generated as described previously (31). The bound primary antibodies were detected with the appropriate peroxidase-conjugated secondary antimouse or antirabbit antibodies (Jackson ImmunoResearch Laboratories, West Grove, PA) and then visualized by chemiluminescence (ECL-Plus; GE Healthcare, Mississauga, Ontario, Canada) and exposure to x-ray films (Eastman Kodak Co., Rochester, NY).

Statistical analysis

Data points represent mean ± SEM. An unpaired Student's *t* test or a one-way ANOVA followed by a Student-Newman-Keuls test was used to compare control values from NB598-treated groups. $P < 0.05$ was used to denote statistical significance.

Results

Inhibition of squalene epoxidase significantly decreases cholesterol levels in β-cells

Cholesterol biosynthesis is initiated from the reduction of 3-hydroxy-3-methylglutaryl coenzyme A, undergoing over 30 steps until the final cholesterol product. 3-Hydroxy-3-methylglutaryl coenzyme A reductase is an inhibition target for clinically used statins. However, inhibition of this enzyme has numerous side effects due to the blockade of secondary synthetic pathways upstream from cholesterol biosynthesis (24). Squalene epoxidase is the second enzyme in committed sterol biosynthesis, and inhibition of this enzyme affects only cholesterol synthesis. To confirm the cholesterol synthesis pathway in pancreatic β-cells, we first determined the expression of squalene epoxidase. RT-PCR detected the mRNA transcripts of this enzyme in pancreatic islets from rat, mouse, and human as well as the clonal INS-1 and MIN6 β-cells (Fig. 1A). The squalene epoxidase inhibitor, NB598, was used to reduce endogenous cholesterol biosynthesis in β-cells (32). The inhibition efficiency of this compound on cholesterol biosynthesis was then examined in β-cells. Delipidated FBS was used for this and subsequent protocols to prevent uptake of cholesterol (*i.e.* lipoproteins) normally found in FBS. Incubation with 10 μM NB598 for 48 h caused a 36 ± 7% reduction in total cholesterol level of MIN6 cells ($n = 6$, $P < 0.01$) (Fig. 1B). A similar reduction in total cholesterol content in mouse and human islets was observed: 40 ± 16% ($n = 4$, $P < 0.05$) and 52 ± 1% ($n = 4$, $P < 0.01$), respectively (Fig. 1B). To further examine the inhibitory effect of NB598 on cholesterol levels in different cellular compartments, we isolated PMs, ER, and insulin SGs from MIN6 cells. NB598 caused a significant decrease in cholesterol by 49 ± 2%, 46 ± 7%, and 48 ± 2% from PM, ER, and SG, respectively ($n = 3$, $P < 0.05$) (Fig. 1C). This demonstrates comparable reduction in cholesterol reduction throughout the cell.

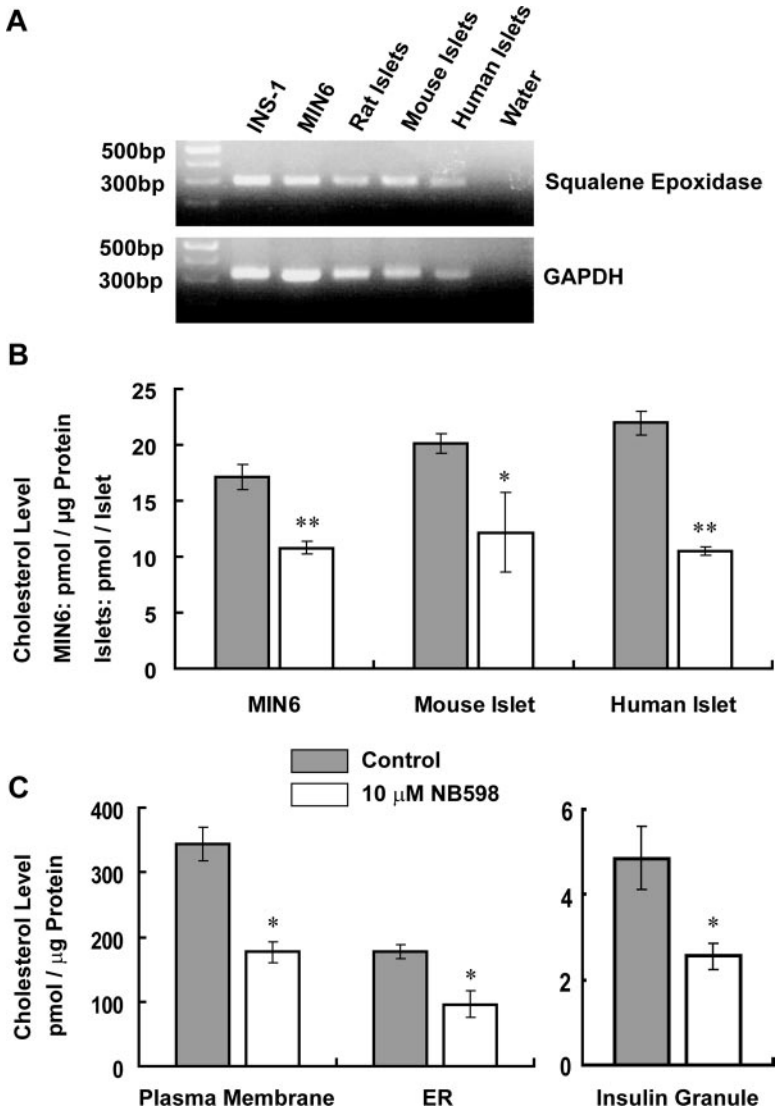

FIG. 1. Inhibition of squalene epoxidase significantly decreases endogenous cholesterol levels in β-cells. A, RT-PCR detected the mRNA transcripts of the committed cholesterol biosynthesis enzyme squalene epoxidase in INS-1 and Min6 β-cells as well as in pancreatic islets from rat, mouse, and human. *Lower panel* shows the glyceraldehyde-3-phosphate dehydrogenase (GAPDH) loading control. B, MIN6 cells, mouse and human islets were cultured with and without 10 μM NB598 for 48 h, and total cholesterol was extracted with chloroform-methanol and measured using a fluorescence assay kit. The squalene epoxidase inhibitor NB598 significantly decreased the cholesterol levels from MIN6 cells, mouse islets, and human islets (*, $P < 0.05$; **, $P < 0.01$, compared with control). C, Cholesterol levels of PMs, ER, and insulin SGs from MIN6 cells. Incubation of the cells with 10 μM NB598 for 48 h caused a significant decrease in cholesterol levels in the respective subcellular compartments (*, $P < 0.05$, compared with control).

Inhibition of cholesterol biosynthesis perturbs insulin secretion from mouse islets

The effect of inhibiting endogenous cholesterol on β-cell function was first examined by glucose-stimulated insulin secretion of mouse islets. Pancreatic islets isolated from MIP-GFP mice were incubated for 48 h with and without NB598. Before all experiments, pancreatic islets or dispersed islet cells were washed thoroughly to minimize any possible direct effects of the compound. NB598 was found to dose-dependently inhibit insulin secretion under both basal (1 mM glucose) and glucose-stimulated (16.7 mM glucose) conditions (Fig. 2). NB598 (2 and 10 μM) caused reductions in basal insulin secretion by 36% (n = 9, $P < 0.01$) and 51% (n = 9, $P < 0.001$), respectively, compared with control. The glucose-stimulated insulin secretion was reduced by 34% (n = 9, $P < 0.01$) and 75% (n = 9, $P < 0.001$) under the same concentrations of NB598, respectively (Fig. 2A). To preclude the possible direct effect of NB598 on insulin synthesis, we also measured the total insulin content of pancreatic islets. NB598 at all doses used for the above insulin secretion studies did no cause any change in the total insulin content of the islets (Fig. 2B). To examine the specificity of NB598 on insulin secretion, we overloaded cholesterol to the NB598-treated cells by incubation with 10 mM soluble cholesterol at 37 C for 1 h (33). Insulin secretion at low glucose condition was fully restored by cholesterol repletion, whereas glucose-stimulated insulin secretion was restored by 57% (n = 6, $P < 0.01$), compared with control (n = 3).

To study the ultrastructure of insulin secretory granules, electron microscopic analysis was performed on mouse islets cultured for 48 h without and with NB598. No gross change in the insulin granule size or density was observed (Fig. 3). These results suggest that the observed impaired insulin secretion by NB598 is the result of a deficiency in cellular cholesterol unrelated to changes in insulin content or granule morphology. Because ion channels and SNARE proteins play an essential role on β-cell stimulus-secretion

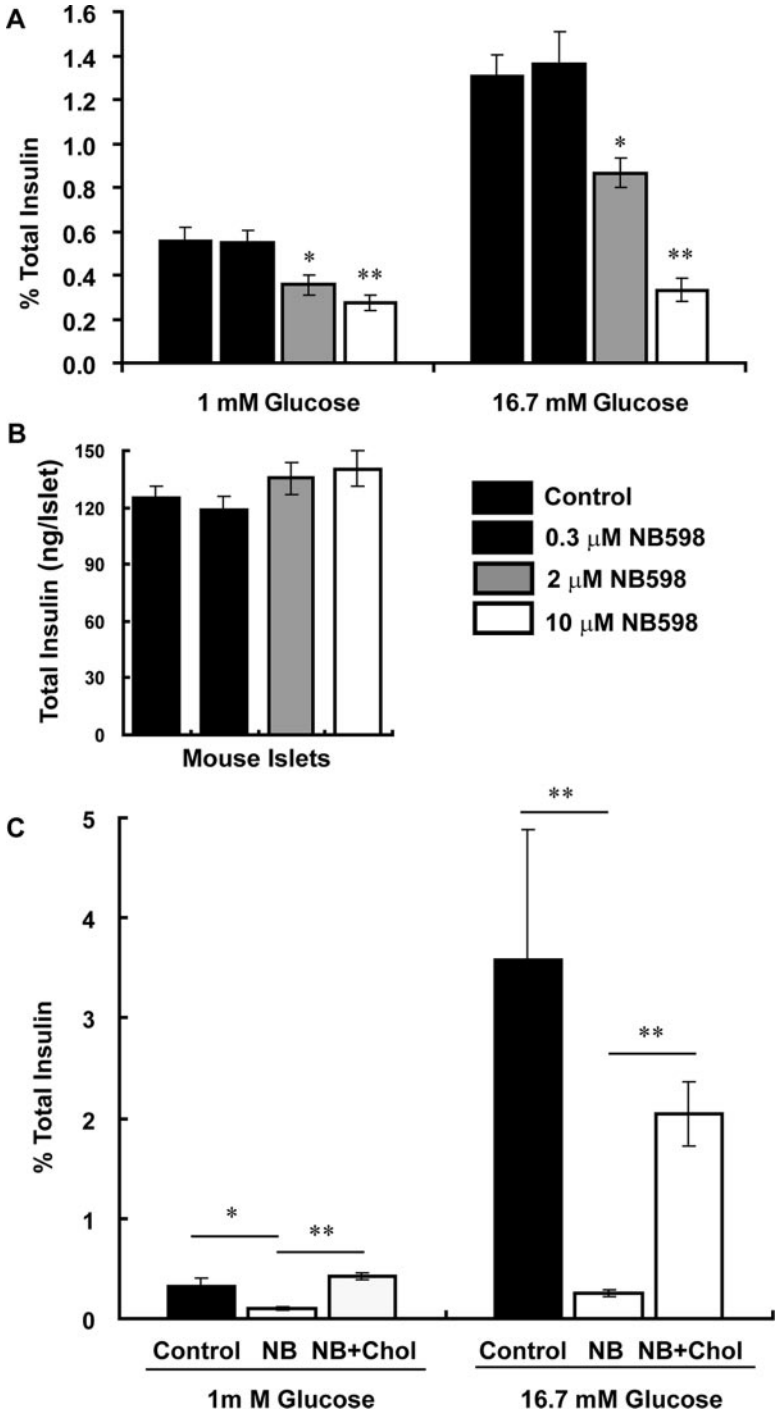

FIG. 2. Inhibition of cholesterol synthesis perturbs insulin secretion from mouse islets. Pancreatic islets isolated from MIP-GFP mice were incubated for 48 h without and with increasing doses of squalene epoxidase inhibitor NB598. Basal insulin secretion (1 mM glucose) and glucose stimulated-insulin secretion (16.7 mM glucose) were measured. A, NB598 dose-dependently inhibits insulin secretion from mouse islets under both basal and high-glucose conditions (*, $P < 0.01$; **, $P < 0.001$, compared with controls). B, Total insulin of mouse islets was measured from the same samples corresponding to A. NB598 does not cause a significant change in total insulin level. C, Insulin secretion measured in mouse islets incubated without or with 10 μM NB 598 alone (NB) or after 1 h incubation with 10 mM soluble cholesterol (NB+Chol). Cholesterol overloading fully restored basal insulin secretion at 1 mM glucose and partially restored glucose-stimulated insulin secretion (*, $P < 0.05$; **, $P < 0.01$).

coupling, we next explored the possible changes in channel activity and single-cell exocytosis after endogenous inhibition of cholesterol biosynthesis by NB598.

Inhibition of cholesterol biosynthesis blocks Ca_V channels

Opening of Ca_V channels and the subsequent increase in $[Ca^{2+}]_i$ are critical to trigger insulin secretion. We previously detected the association of Ca_V channels with cholesterol-rich membrane rafts in pancreatic β-cells (22). Therefore, impairment of insulin secretion caused by the inhibition of cholesterol production by NB598 could be mediated by the altered Ca_V channel activity. Dispersed islet cells from MIP-GFP mice were cultured with different concentrations of NB598 for 48 h, followed by repeated drug washout before electrophysiological measurements were made. The β-cells were identified by the expression of GFP. Consistent with the reduction in insulin secretion, NB598 caused a dose-dependent decrease in Ca_V currents (Fig. 4, A and B). The peak Ca_V current amplitude measured at +10 mV was -13.3 ± 1.0 pA/pF (n = 9) in control cells, -3.7 ± 1.2 pA/pF (n = 4, $P < 0.001$), and

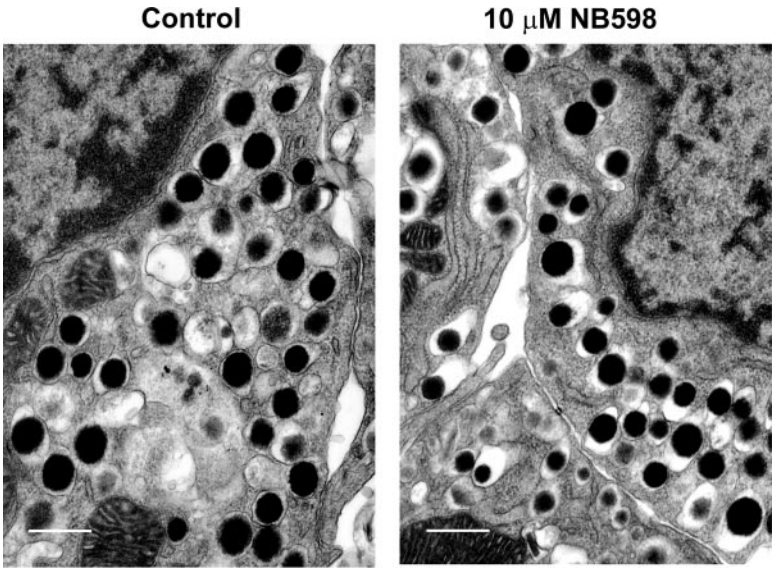

FIG. 3. Electron microscopic analysis of insulin granules. Pancreatic islets isolated from MIP-GFP mice were treated as in Fig. 2. Insulin granules from islets incubated with 10 μM NB598 (*right panel*) displayed similar gross morphology and density as those from control islets (*left panel*). *White scale bar*, 500 nm.

-2.1 ± 0.1 pA/pF (n = 10, $P < 0.001$) in 2 and 10 μM NB598-treated cells, respectively. To preclude any possible direct effects of the drug on Ca_V channels, we added the 10 μM NB598 acutely into the bath solution and observed no effect on Ca_V currents (data not shown). Furthermore, cholesterol repletion experiments restored Ca_V current amplitude to 78% of control (n = 6), which was not statistically different from control (Fig. 4C). We speculate the resultant decrease in Ca_V currents after cholesterol reduction is one of the primary mediators for the observed inhibition of insulin secretion by NB598.

NB598 increases K_V channel inactivation

K_V channels regulate membrane potential repolarization and finely tune insulin secretion (2). We reported that $K_V2.1$ channels are associated with lipid raft domains in β-cells, and the currents are regulated by the surrounding lipid environment (22). NB598 at concentrations up to 10 μM did not affect peak outward K_V currents or the voltage dependence of activation (data not shown) but increased current inactivation (Fig. 5A). A longer (12 sec) depolarization at +70 mV was performed to clearly display this inactivation effect on K_V channels. Increasing concentrations of NB598 accelerated the inactivation rate of K_V channels (Fig. 5B). Steady-state inactivation was measured after a 5-sec conditioning depolarization from −120 mV to +20 mV followed by 500-msec test steps at +60 mV. No hyperpolarizing shift in the steady-state inactivation curve was observed, but the slope factor decreased from 15.4 ± 1.2 mV (control) to 9.2 ± 0.7 mV (10 μM NB598 treated cells; n = 4, $P < 0.01$) (Fig. 5C). Furthermore, the relative amount of noninactivating current was significantly different. Control cells displayed $45 \pm 1\%$ noninactivating K_V current at 0 mV (n = 4), whereas cells cultured with 10 μM NB598 displayed only $11 \pm 1\%$ noninactivating K_V currents (n = 4; $P < 0.05$) (Fig. 5C). Cholesterol

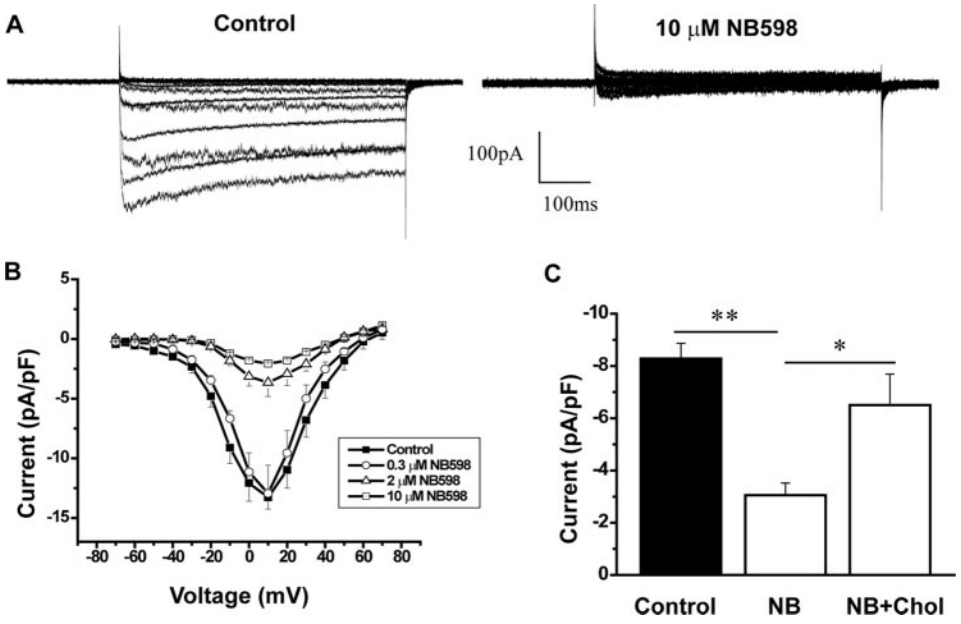

FIG. 4. NB598 inhibits mouse β-cell Ca_V channels. Pancreatic islet cells isolated from MIP-GFP mice were incubated for 48 h without and with increasing doses of NB598. β-Cells were recognized by GFP marker. A, Representative traces showing Ca^{2+} currents triggered by a series of pulses (from −70 to +70 mV, 500 msec) from a holding potential of −80 mV in a control β-cell and a β-cell treated with 10 μM NB598, indicating a significant inhibition of Ca_V currents by 10 μM NB598. B, Current-voltage relationship of Ca_V channels under different concentrations of squalene epoxidase inhibitor NB598; 2 μM ($P < 0.001$) and 10 μM NB598 ($P < 0.001$) dose-dependently inhibited Ca_V currents at depolarizing voltages from −40 mV to +50 mV. C, Peak Ca_V currents at −10 mV for β-cells treated without or with 10 μM NB598 alone (NB) or after 1 h incubation with 10 mM soluble cholesterol (NB+Chol) before recording. Cholesterol repletion significantly restored the decreased Ca_V currents (*, $P < 0.05$; **$P < 0.001$).

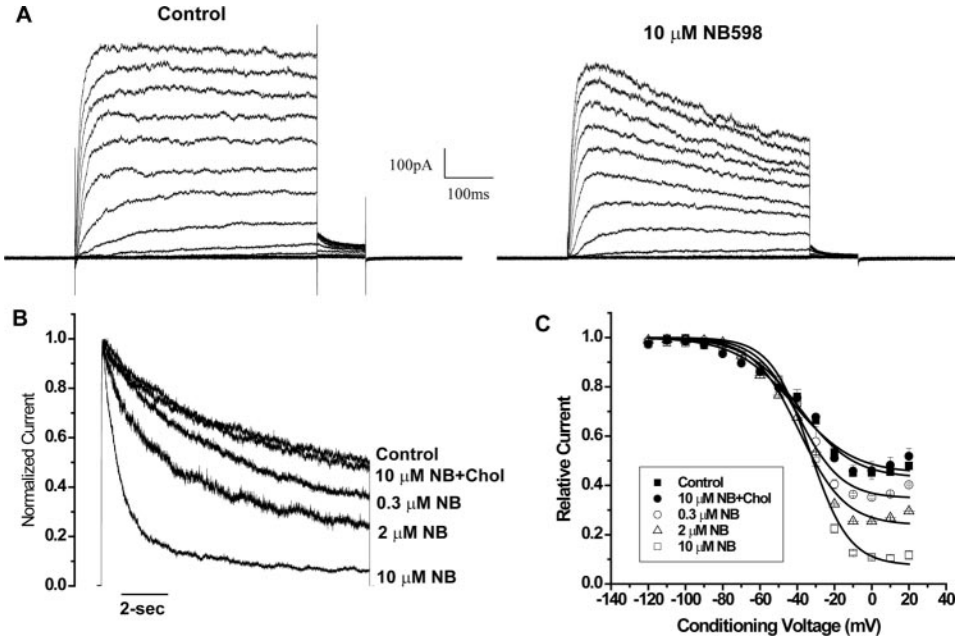

FIG. 5. NB598 increases the steady-state inactivation of K_V channels in mouse β-cells. Pancreatic β-cells from MIP-GFP mice were held at −80 mV, and whole-cell K_V currents were measured after depolarization from −80 to +60 mV in 10-mV increments using 500-msec step pulses. A, Representative traces of K_V currents from a control β-cell and a β-cell cultured for 48 h in the presence of 10 μM NB598, demonstrating that NB598 does not affect peak K_V currents but enhances current inactivation. B, Longer depolarizations (12 sec) at +70 mV were performed to display this inactivation effect. Increasing concentrations of NB598 accelerated the inactivation rate of K_V channels. The effect of 10 μM NB598 treatment on K_V current inactivation was fully reversed after 1 h cholesterol repletion with 10 mM soluble cholesterol (10 μM NB + Chol). C, Steady-state inactivation of K_V channels was measured after 5-sec conditioning depolarization pulses at voltages from −120 mV to +20 mV. No left shift in the steady-state inactivation curve was observed, but the slope factors for all NB598 doses decreased ($P < 0.01$). The relative amount of noninactivating current measured at 0 mV was also significantly decreased from cells cultured with NB598 ($P < 0.05$). The inactivation curve fully recovered after cholesterol repletion (10 μM NB + Chol).

repletion fully restored the inactivated K_V currents (Fig. 5, B and C), confirming that the effect of NB598 on K_V channels was a result of reduced membrane cholesterol levels. Besides K_V channels, 10 μM NB598 also decreased K_{ATP} current density at −140 mV by 57 ± 4% (n = 7, $P < 0.01$, data not shown). However, we do not believe the changes in either K_V or K_{ATP} channels played a role on the reduced insulin release observed above because it has been well established that reductions in either K_V or K_{ATP} currents enhance insulin secretion (2, 34, 35).

Inhibition of cholesterol biosynthesis by NB598 impairs β-cell exocytosis

We next investigated the effects of NB598 pretreatment on β-cell exocytosis. To exclude the dependency of Ca^{2+} influx from Ca^{2+} channels, exocytosis was elicited by flash photolysis of caged Ca^{2+} (NP-EGTA) (9). Exocytosis was monitored as an increase in whole-cell Cm. In response to the step-like elevation in $[Ca^{2+}]_i$ generated by the uncaging of Ca^{2+} by flash photolysis, capacitance traces displayed a rapid, burst-like increase within the first 0.5 sec after the flash followed by a slower sustained phase of exocytosis. Changes in Cm consisted of three components, which have been termed the fast burst, slow burst, and sustained components (12, 36). The fast and slow burst components are generally interpreted as the fusion of docked and primed vesicles from the rapidly and slowly releasable pools, respectively, whereas the sustained component represents refilling of the releasable pools from a large depot pool of vesicles (37). In our experiments, flash photolysis of NP-EGTA induced a step-like homogenous increase in $[Ca^{2+}]_i$ from 200 to 300 nM to 5–10 μM. The averaged Cm traces were compared from control and NB598-treated cells responding to similar step-like $[Ca^{2+}]_i$ elevations (Fig. 6). The amplitude of the fast burst in NB598-treated cells was reduced from 282 ± 30 femtofarad (fF) (control) to 212 ± 16 fF but was not significantly different. However, there was a dramatic reduction in the size of the slow burst component from 513 ± 42 fF (control) to 158 ± 3 fF ($P < 0.01$) in NB598-treated cells. Furthermore, we also observed a significant decrease in the sustained component. The amplitude of the sustained component from NB598-treated cells was 192 ± 27 *vs.* 365 ± 30 fF in control cells. These results suggest that inhibition of cholesterol synthesis with NB598 markedly impaired β-cell exocytosis from both fusion vesicle pool and refilling of releasable pool.

Cholesterol inhibition causes redistribution of membrane raft-associated ion channels and SNARE proteins

To further determine the molecular mechanism of the impaired function of ion channels and insulin exocytosis, we examined whether the effects of NB598 were caused by changes in protein expression and/or membrane distribution of those corresponding ion channels and SNARE proteins. MIN6 β-cells were cultured for 48 h in the absence and presence of 10 μM NB598, and protein expression was de-

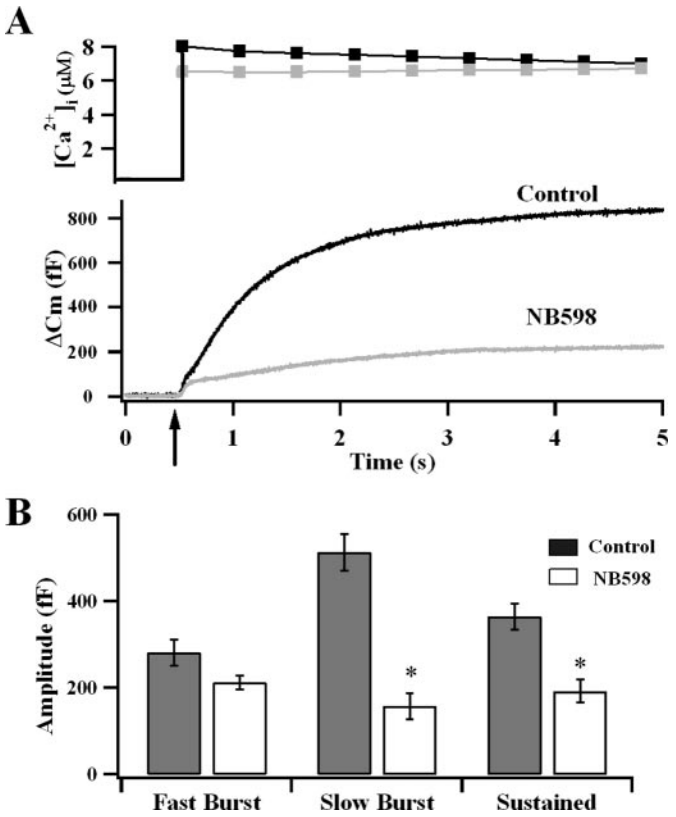

FIG. 6. NB598 inhibits β-cell exocytosis independently of Ca_V channels. Exocytosis was elicited by flash photolysis and was monitored by whole-cell membrane capacitance measurement. Treatment with 10 μM NB598 powerfully reduced exocytosis from mouse pancreatic β-cells. A, Averaged $[Ca^{2+}]_i$ and capacitance changes from control (*black bars*) and 10 μM NB598-treated (*gray bars*) cells. *Arrow* indicates the initial flash. Capacitance increase in the cells treated with 10 μM NB598 is significantly inhibited, compared with control cells, indicating an inhibition of NB598 on β-cell exocytosis independently from Ca_V channels. B, Mean amplitudes of the exocytotic burst and sustained components from control (*gray bars*) and 10 μM NB598-treated (*white bars*) cells, respectively. The Cm response was fitted with a triple exponential function, and the amplitudes of the two fast components were taken as the size of the fast burst and slow burst components, respectively. The slow component represents the sustained phase of secretion. NB598 inhibited both slow burst and sustained components of exocytosis, indicating the inhibition of cholesterol synthesis affects not only the release of docked and primed granules but also the refilling of granules. *, $P < 0.01$, compared with control.

termined by Western blot analysis. NB598 treatment did not have any significant effect on the protein expression of the channel proteins $Ca_V1.2$ or $K_V2.1$ and the SNARE proteins syntaxin 1A, SNAP-25, and VAMP-2 (data not shown). Discontinuous sucrose gradient centrifugation of MIN6 cell lysate incubated with Triton X-100 at 4 C was used to detect protein targeting to membrane raft fractions (22, 23). We observed a redistribution of $Ca_V1.2$, $K_V2.1$, syntaxin1A, SNAP-25, and VAMP-2 out of the cholesterol-rich membrane raft fraction located at the interface of 5 and 30% sucrose (Fig. 7).

Discussion

Cholesterol is important in the organization of lipid bilayers, and the disorders of cholesterol can cause severe consequences (38). The majority of studies examining the role

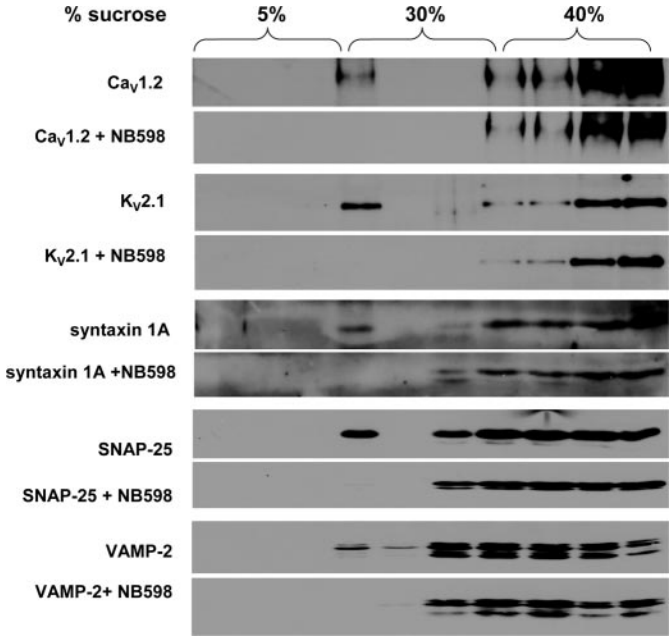

FIG. 7. Inhibition of cholesterol causes redistribution of ion channels and SNARE proteins from cholesterol-rich membrane raft microdomains. MIN6 β-cells were cultured for 48 h without and with 10 μM NB598. Localization of ion channels and SNARE proteins to membrane rafts was characterized by sucrose gradient ultracentrifugation and subsequent Western blot analysis. The interface between 5 and 30% sucrose gradient denotes the membrane raft fraction. Ca_V and K_V channels and the SNARE proteins syntaxin 1A, SNAP-25, and VAMP-2 were found to be associated with cholesterol-rich membrane rafts in MIN6 cells. Inhibition of cholesterol synthesis with NB598 caused redistribution of those ion channels and SNARE proteins from the membrane rafts.

of cholesterol-rich membrane rafts have been based on acute cholesterol depletion with MβCD, a commonly used chemical that can effectively sequester cholesterol from PMs (39). However, because MβCD is membrane impermeable, treatment of cells with MβCD is expected to only deplete cholesterol and disrupt membrane rafts on the outer leaflet of the PM. Alternatively, it has also been suggested that cholesterol depletion with MβCD may affect intracellular cholesterol stores due to the rapid trafficking and efflux of cholesterol to the PM (33). However, the short incubation (30 min) used in our previous study may not have been long enough to cause an efficient depletion of intracellular cholesterol. The present study illustrates that chronic inhibition of cholesterol biosynthesis reduces cholesterol at the PMs as well as the intracellularly ER and insulin secretory granular membranes. Therefore, inhibition of endogenous cholesterol could lead to a more profound interference of cellular structure and function, resulting in alterations in β-cell stimulus-secretion coupling.

Cholesterol is synthesized in the ER and transported to the PMs via two pathways (40). The major pathway is via energy-dependent nonvesicular transport against a concentration gradient (41). About 20% of the *de novo* synthesized cholesterol is transported to PMs through vesicular transport via the Golgi apparatus (42). Although this vesicular pathway is not a major route of cholesterol export, some cholesterol exported from the ER may become confined to lipid rafts before reaching the PMs (42). Therefore, the passage of cholesterol through the ER-Golgi apparatus might play an important role in raft-dependent sort-

ing of proteins (43, 44). Inhibition of endogenous cholesterol biosynthesis may cause an inappropriate protein sorting of membrane proteins such as ion channels and SNARE proteins in pancreatic β-cells. Therefore, the impaired function of ion channels and exocytosis caused by the inhibition of endogenous cholesterol biosynthesis by NB598 could be a result of the disruption of cholesterol in not only the PMs but also the ER and insulin secretory granules.

Roles of endogenous cholesterol in regulating K_V channel function

Inhibition of squalene epoxidase significantly increased the inactivation of K_V channels in β-cells but did not affect current density or the voltage dependence of channel activation. K_V channel inactivation is described by a ball-and-chain model, a process by which the N-terminal cytoplasmic domain of $K_V\alpha$ or $K_V\beta$ subunit occludes the inner open channel pore (45). This cytoplasmic domain of K_V channels was found to interact strongly with membrane lipids. K_V channels, as well as other ion channels, are regulated by the lipid composition of PMs (46). Modulation of membrane lipids have been shown to result in rapid inactivation (A-type currents) of noninactivating K_V channels and, conversely, endow noninactivating delayed rectifying properties to A-type K_V currents (47). Inhibiting endogenous cholesterol biosynthesis could have profoundly altered the membrane lipid composition, channel-lipid interaction, and conformational changes of the channel proteins, all of which could have contributed to the observed enhancement of K_V channel inactivation by NB598. The consequence of enhanced inactivation of K_V channels on β-cell function remains to be further investigated. However, we speculate these effects do not contribute to the observed inhibition on insulin secretion because inhibition of K_V channels are known to enhance insulin secretion (2, 35).

Role of endogenous cholesterol on β-cell exocytotic machinery

Chronic cholesterol synthesis inhibition markedly reduced Ca_V currents and insulin secretion. The link between the inhibition of cholesterol synthesis and the impairment in Ca_V channel function is not clear. No effect of NB598 on the protein expression of Ca_V channels was observed. The decreased Ca_V currents could be caused by a possible inappropriate membrane localization of the Ca_V channels out of membrane rafts or changes in the interactions of the different auxiliary Ca_V channel subunits. Second, reduced membrane cholesterol may lead to conformational changes of the channel protein due to disruption of the channel-lipid interaction as we suggest may be occurring with K_V channels.

SNARE proteins constitute the core of exocytotic machinery in neuroendocrine cells and are critical for the release of neurotransmitter and hormone. Recent studies implicate that cholesterol-rich membrane rafts could play an important role in regulated exocytosis through compartmentalizing SNARE proteins at defined sites on the plasma membrane. We and others have previously shown that the SNARE proteins syntaxin1A, SNAP-25, and VAMP-2 are associated with cholesterol-rich membrane rafts in pancreatic β- and α-cells (22, 23, 48, 49). The t-SNAREs syntaxin 1 and SNAP-25 were found both to cluster in plasma membrane in β-cells and PC12 cells, and their integrity is dependent on membrane cholesterol (48–51). Therefore, cholesterol being a major constituent of membrane rafts could play an essential role in regulating exocytosis through maintaining the function of secretory machinery. Single-cell membrane capacitance measurement indicated that NB958 treatment impaired exocytosis independently from the dysfunction of Ca_V channels. Cholesterol could regulate exocytosis through protein accumulation or exclusion in the membrane raft domains or reduce the energetic barrier for vesicular-plasma membrane lipid fusion (52).

We were initially surprised by our observations in this study because they are in contrast to our previous work (22), in which we observed acute membrane cholesterol depletion with MβCD did not affect Ca_V currents and enhanced insulin secretion. We concluded in the previous study that the enhanced insulin secretion could be partially mediated by the strong inhibition of the amplitude of the K_V channels and effects on the exocytic machinery. However, it is not unexpected that acute and chronic manipulations in membrane cholesterol could elicit markedly different cellular changes. Inhibiting cholesterol synthesis would affect membrane cholesterol, as well as cholesterol-mediated processes. Cholesterol and cholesterol-interacting proteins (*e.g.* caveolin) regulate the trafficking and targeting of proteins, including ion channels, to membrane rafts (53, 54) and are important in coordinating the assembly of calcium channels with SNARE proteins in the exocytotic domains (55, 56). Given these possible explanations, we were even more astonished that acute cholesterol repletion restored much of the defects in Ca_V channel activity and insulin secretion. Therefore, further investigations are warranted into determining the precise mechanisms mediating the alterations in channel activity and exocytosis after chronic cholesterol depletion.

In summary, we have demonstrated a critical role for endogenous cholesterol in the normal function of pancreatic β-cells. Using NB598, a cholesterol biosynthesis inhibitor, we found there are two major roles that endogenous cholesterol may play in β-cell exocytosis. First, endogenous cholesterol maintains normal function of Ca_V channels. Second, cholesterol is critical in the mobilization and fusion of insulin granules with plasma membranes. Dysregulation of cellular cholesterol may cause impairment in β-cell function, a possible pathogenesis leading to the development of type 2 diabetes.

Acknowledgments

Received February 5, 2008. Accepted June 25, 2008.

Address all correspondence and requests for reprints to: Robert G. Tsushima, Department of Biology, York University, 4700 Keele Street, Farquharson 344, Toronto, Ontario, Canada M3J 1P3. E-mail: tsushima@yorku.ca.

This work was supported by grants and fellowships from the Canadian Institutes of Health Research (MOP 77638, to R.G.T.; MOP-69083, to H.Y.G. and R.G.T.), and equipment grants from James H. Cummings Foundation, J.P. Bickell Foundation, the Banting and Best Diabetes Centre (BBDC). F.X. was supported by an Ontario Graduate Scholarship, BBDC Studentship, and Canadian Diabetes Association Doctoral Studentship Research Award.

Current address for Y.C.: Central Laboratory, Guangzhou Children's Hospital, Guangzhou 510120, Guangdong, China.

Current address for R.G.T.: Department of Biology, York University, Toronto, Ontario M3J 1P3, Canada.

Disclosure Statement: F.X., L.X., A.M., X.G., Y.C., H.Y.G., and R.G.T. have nothing to declare.

References

1. **Rorsman P, Renstrom E** 2003 Insulin granule dynamics in pancreatic β cells. Diabetologia 46:1029–1045
2. **Macdonald PE, Ha XF, Wang J, Smukler SR, Sun AM, Gaisano HY, Salapatek AM, Backx PH, Wheeler MB** 2001 Members of the Kv1 and Kv2 voltage-dependent K^+ channel families regulate insulin secretion. Mol Endocrinol 15:1423–1435
3. **Barg S, Ma X, Eliasson L, Galvanovskis J, Gopel SO, Obermuller S, Platzer J, Renstrom E, Trus M, Atlas D, Striessnig J, Rorsman P** 2001 Fast exocytosis with few Ca^{2+} channels in insulin-secreting mouse pancreatic β cells. Biophys J 81:3308–3323
4. **Brunger AT** 2000 Structural insights into the molecular mechanism of Ca^{2+}-dependent exocytosis. Curr Opin Neurobiol 10:293–302
5. **Li L, Chin LS** 2003 The molecular machinery of synaptic vesicle exocytosis. Cell Mol Life Sci 60:942–960
6. **Bruns D, Jahn R** 2002 Molecular determinants of exocytosis. Pflugers Arch 443:333–338
7. **Weber T, Zemelman BV, McNew JA, Westermann B, Gmachl M, Parlati F, Sollner TH, Rothman JE** 1998 SNAREpins: minimal machinery for membrane fusion. Cell 92:759–772
8. **Curry DL, Bennett LL, Grodsky GM** 1968 Dynamics of insulin secretion by the perfused rat pancreas. Endocrinology 83:572–584
9. **Neher E** 1998 Vesicle pools and Ca^{2+} microdomains: new tools for understanding their roles in neurotransmitter release. Neuron 20:389–399
10. **Rorsman P, Eliasson L, Renstrom E, Gromada J, Barg S, Gopel S** 2000 The cell physiology of biphasic insulin secretion. News Physiol Sci 15:72–77
11. **Rettig J, Neher E** 2002 Emerging roles of presynaptic proteins in Ca^{2+}-triggered exocytosis. Science 298:781–785
12. **Xu T, Rammner B, Margittai M, Artalejo AR, Neher E, Jahn R** 1999 Inhibition of SNARE complex assembly differentially affects kinetic components of exocytosis. Cell 99:713–722
13. **Ostenson CG, Gaisano H, Sheu L, Tibell A, Bartfai T** 2006 Impaired gene and protein expression of exocytotic soluble *N*-ethylmaleimide attachment protein receptor complex proteins in pancreatic islets of type 2 diabetic patients. Diabetes 55:435–440
14. **Chan CB, MacPhail RM, Sheu L, Wheeler MB, Gaisano HY** 1999 β-Cell hypertrophy in fa/fa rats is associated with basal glucose hypersensitivity and reduced SNARE protein expression. Diabetes 48:997–1005
15. **Gaisano HY, Ostenson CG, Sheu L, Wheeler MB, Efendic S** 2002 Abnormal expression of pancreatic islet exocytotic soluble *N*-ethylmaleimide-sensitive factor attachment protein receptors in Goto-Kakizaki rats is partially restored by phlorizin treatment and accentuated by high glucose treatment. Endocrinology 143: 4218–4226
16. **Ohara-Imaizumi M, Nishiwaki C, Kikuta T, Nagai S, Nakamichi Y, Nagamatsu S** 2004 TIRF imaging of docking and fusion of single insulin granule motion in primary rat pancreatic β-cells: different behaviour of granule motion between normal and Goto-Kakizaki diabetic rat β-cells. Biochem J 381:13–18
17. **Haines TH** 2001 Do sterols reduce proton and sodium leaks through lipid bilayers? Prog Lipid Res 40:299–324
18. **Ohvo-Rekila H, Ramstedt B, Leppimaki P, Slotte JP** 2002 Cholesterol interactions with phospholipids in membranes. Prog Lipid Res 41:66–97
19. **Inokuchi J** 2006 Insulin resistance as a membrane microdomain disorder. Biol Pharm Bull 29:1532–1537
20. **Michel V, Bakovic M** 2007 Lipid rafts in health and disease. Biol Cell 99:129–140
21. **Parton RG** 2003 Caveolae—from ultrastructure to molecular mechanisms. Nat Rev Mol Cell Biol 4:162–167
22. **Xia F, Gao X, Kwan E, Lam PP, Chan L, Sy K, Sheu L, Wheeler MB, Gaisano HY, Tsushima RG** 2004 Disruption of pancreatic β-cell lipid rafts modifies Kv2.1 channel gating and insulin exocytosis. J Biol Chem 279:24685–24691
23. **Xia F, Leung YM, Gaisano G, Gao X, Chen Y, Manning Fox JE, Bhattacharjee A, Wheeler MB, Gaisano HY, Tsushima RG** 2007 Targeting of KV4, CaV1.2 and SNARE proteins to cholesterol-rich lipid rafts in pancreatic α-cells: effects on glucagon stimulus-secretion coupling. Endocrinology 148:2157–2167
24. **Chugh A, Ray A, Gupta JB** 2003 Squalene epoxidase as hypocholesterolemic drug target revisited. Prog Lipid Res 42:37–50
25. **Shapiro AM, Lakey JR, Ryan EA, Korbutt GS, Toth E, Warnock GL, Kneteman NM, Rajotte RV** 2000 Islet transplantation in seven patients with type 1 diabetes mellitus using a glucocorticoid-free immunosuppressive regimen. N Engl J Med 343:230–238
26. **Ramanadham S, Bohrer A, Gross RW, Turk J** 1993 Mass spectrometric characterization of arachidonate-containing plasmalogens in human pancreatic islets and in rat islet β-cells and subcellular membranes. Biochemistry 32:13499–13509
27. **Brunner Y, Coute Y, Iezzi M, Foti M, Fukuda M, Hochstrasser DF, Wollheim CB, Sanchez JC** 2007 Proteomics analysis of insulin secretory granules. Mol Cell Proteomics 6:1007–1017
28. **Leung YM, Ahmed I, Sheu L, Tsushima RG, Diamant NE, Hara M, Gaisano HY** 2005 Electrophysiological characterization of pancreatic islet cells in the mouse insulin promoter-green fluorescent protein mouse. Endocrinology 146:4766–4775
29. **Xu T, Binz T, Niemann H, Neher E** 1998 Multiple kinetic components of exocytosis distinguished by neurotoxin sensitivity. Nat Neurosci 1:192–200
30. **Grynkiewicz G, Poenie M, Tsien RY** 1985 A new generation of Ca^{2+} indicators with greatly improved fluorescence properties. J Biol Chem 260:3440–3450
31. **Wheeler MB, Sheu L, Ghai M, Bouquillon A, Grondin G, Weller U, Beaudoin AR, Bennett MK, Trimble WS, Gaisano HY** 1996 Characterization of SNARE protein expression in β cell lines and pancreatic islets. Endocrinology 137:1340–1348
32. **Horie M, Tsuchiya Y, Hayashi M, Iida Y, Iwasawa Y, Nagata Y, Sawasaki Y, Fukuzumi H, Kitani K, Kamei T** 1990 NB-598: a potent competitive inhibitor of squalene epoxidase. J Biol Chem 265:18075–18078
33. **Hao M, Head WS, Gunawardana SC, Hasty AH, Piston DW** 2007 Direct effect of cholesterol on insulin secretion: a novel mechanism for pancreatic β-cell dysfunction. Diabetes 56:2328–2338
34. **Ashcroft FM** 2005 ATP-sensitive potassium channelopathies: focus on insulin secretion. J Clin Invest 115:2047–2058
35. **Macdonald PE, Sewing S, Wang J, Joseph JW, Smukler SR, Sakellaropoulos G, Wang J, Saleh MC, Chan CB, Tsushima RG, Salapatek AM, Wheeler MB** 2002 Inhibition of Kv2.1 voltage-dependent K^+ channels in pancreatic β-cells enhances glucose-dependent insulin secretion. J Biol Chem 277:44938–44945
36. **Voets T, Neher E, Moser T** 1999 Mechanisms underlying phasic and sustained secretion in chromaffin cells from mouse adrenal slices. Neuron 23:607–615
37. **Sorensen JB** 2004 Formation, stabilisation and fusion of the readily releasable pool of secretory vesicles. Pflugers Arch 448:347–362
38. **Maxfield FR, Tabas I** 2005 Role of cholesterol and lipid organization in disease. Nature 438:612–621
39. **Christian AE, Haynes MP, Phillips MC, Rothblat GH** 1997 Use of cyclodextrins for manipulating cellular cholesterol content. J Lipid Res 38:2264–2272
40. **Maxfield FR, Wustner D** 2002 Intracellular cholesterol transport. J Clin Invest 110:891–898
41. **Chang TY, Chang CC, Ohgami N, Yamauchi Y** 2006 Cholesterol sensing, trafficking, and esterification. Annu Rev Cell Dev Biol 22:129–157
42. **Heino S, Lusa S, Somerharju P, Ehnholm C, Olkkonen VM, Ikonen E** 2000 Dissecting the role of the Golgi complex and lipid rafts in biosynthetic transport of cholesterol to the cell surface. Proc Natl Acad Sci USA 97: 8375–8380
43. **Simons K, Ikonen E** 1997 Functional rafts in cell membranes. Nature 387:569–572
44. **Helms JB, Zurzolo C** 2004 Lipids as targeting signals: lipid rafts and intracellular trafficking. Traffic 5:247–254
45. **Zagotta WN, Hoshi T, Aldrich RW** 1990 Restoration of inactivation in mutants of Shaker potassium channels by a peptide derived from ShB. Science 250:568–571
46. **Hilgemann DW** 2004 Biochemistry. Oily barbarians breach ion channel gates. Science 304:223–224
47. **Oliver D, Lien CC, Soom M, Baukrowitz T, Jonas P, Fakler B** 2004 Functional conversion between A-type and delayed rectifier K^+ channels by membrane lipids. Science 304:265–270
48. **Ohara-Imaizumi M, Nishiwaki C, Kikuta T, Kumakura K, Nakamichi Y, Nagamatsu S** 2004 Site of docking and fusion of insulin secretory granules in live MIN6 β cells analyzed by TAT-conjugated anti-syntaxin 1 antibody and total internal reflection fluorescence microscopy. J Biol Chem 279: 8403–8408
49. **Takahashi N, Hatakeyama H, Okado H, Miwa A, Kishimoto T, Kojima T, Abe T, Kasai H** 2004 Sequential exocytosis of insulin granules is associated with redistribution of SNAP25. J Cell Biol 165:255–262
50. **Chamberlain LH, Burgoyne RD, Gould GW** 2001 SNARE proteins are highly enriched in lipid rafts in PC12 cells: implications for the spatial control of exocytosis. Proc Natl Acad Sci USA 98:5619–5624
51. **Lang T, Bruns D, Wenzel D, Riedel D, Holroyd P, Thiele C, Jahn R** 2001 SNAREs are concentrated in cholesterol-dependent clusters that define docking and fusion sites for exocytosis. EMBO J 20:2202–2213
52. **Churchward MA, Rogasevskaia T, Hofgen J, Bau J, Coorssen JR** 2005 Cholesterol facilitates the native mechanism of Ca^{2+}-triggered membrane fusion. J Cell Sci 118:4833–4848
53. **Kong MM, Hasbi A, Mattocks M, Fan T, O'Dowd BF, George SR** 2007 Regulation of D1 dopamine receptor trafficking and signaling by caveolin-1. Mol Pharmacol 72:1157–1170
54. **Pediconi MF, Gallegos CE, Los Santos EB, Barrantes FJ** 2004 Metabolic cholesterol depletion hinders cell-surface trafficking of the nicotinic acetylcholine receptor. Neuroscience 128:239–249
55. **Cho WJ, Jeremic A, Jin H, Ren G, Jena BP** 2007 Neuronal fusion pore assembly requires membrane cholesterol. Cell Biol Int 31:1301–1308
56. **Nevins AK, Thurmond DC** 2006 Caveolin-1 functions as a novel Cdc42 guanine nucleotide dissociation inhibitor in pancreatic β-cells. J Biol Chem 281:18961–18972

***Endocrinology* is published monthly by The Endocrine Society (http://www.endo-society.org), the foremost professional society serving the endocrine community.**